J Fluoresc (2015) 25:1267–1277
DOI 10.1007/s10895-015-1615-0

ORIGINAL ARTICLE

Fluorescence Detection of Single DNA Molecules

Weidong Huang[1] · **Yue Wang**[1] · **Zhimin Wang**[1]

Received: 20 March 2015 / Accepted: 5 July 2015 / Published online: 28 July 2015

Abstract Single-molecule detection (SMD) and single-molecule fluorescence resonance energy transfer (smFRET) were conducted using Cy3- and Cy5-labeled single-strand DNAs (ssDNAs) either immobilized on substrates or encapsulated in microdroplets. High-quality fluorescent images were obtained using a total internal reflection fluorescence microscope (TIRFM). In the substrate system, deposition of a low concentration of fluorescence molecules on substrates through electrostatic adsorption showed that most of the fluorescence spots were single molecules, and the mean value of signal to noise ratio (S/N) reached 6.9±0.34. smFRET analysis was conducted through immobilization of donor- and acceptor-labeled oligonucleotides on substrates. In the droplet system, fluorophor-labeled oligonucleotides were injected into T-type microfluidics. Single and double fluorophor-labeled DNA molecules encapsulated in droplets were detected, the FRET efficiency and inter-dye distance of a single donor-acceptor pair were measured accurately. smFRET was conducted detailedly in the tortuous channel for the first time.

Keywords Single-molecule detection · TIRFM · Signal to noise ratios · Microdroplet · smFRET

Introduction

Single-molecule detection (SMD) is a powerful tool for analysis of interactions between molecules, exhibiting high sensitivity and specificity compared with ensemble methods. It represents the determination limit and the ultimate goal of analytical chemistry [1–4], and has therefore drawn increasing attention in physics, chemistry, and biology since detection of activity of single-molecule β-D-galactosidase was demonstrated in 1961 [5].

Several microscopies can be applied to detect single molecules. One is epifluorescence microscopy (EFM), which was able to detect single molecules once fluorescence markers with high fluorescence intensity became available [6–8]. Confocal fluorescence microscopy (CFM), a high-resolution microscopic imaging technique, tremendously diminished fluorescence interference adjacent to the observation point, allowing for improved S/N [3, 8–10]. Total internal reflection fluorescence microscopy (TIRFM) is able to generate a thin field of illumination while reducing background signal by generating an evanescent wave within a thickness of less than 200 nm, dramatically. Another technique, stochastic optical reconstruction microscopy (STORM), is a super-resolution technique based on photoswitchable fluorescence molecules and using a focus-lock system. This technique has broken the diffraction limit of optical resolution, and could theoretically achieve precise location of a single molecule [11–14].

Fluorescence resonance energy transfer (FRET) has been widely used to study the dynamics and structure changes of DNA [15, 16], RNA [17, 18], and proteins [19–21] in ensemble measurements. However, the fluorescence signals obtained from ensemble experiments are limited as they reflect the average characteristics of all the molecules, and thus are unable to monitor interactions and comformational changes of individual molecules. To address this limitation, single-molecule fluorescence resonance energy transfer (smFRET) was developed [22]. Samples for SMD could be separated according to their environments, including those in solution [1, 23–25], on substrates [26–28], in cell [29–31], and in droplets [32–36]. Most smFRET studies to date have utilized

✉ Zhimin Wang
zmwang@sjtu.edu.cn

[1] School of Agriculture and Biology, Shanghai Jiao Tong University, Shanghai 200240, China

immobilized samples on substrates tethered through the strong interaction of biotin and streptavidin [37–40], while there are fewer studies using samples in microdroplets [41].

In this report, we conducted SMD and smFRET using samples either immobilized on substrates or encapsulated in microdroplets under a TIRFM system. Dye-labeled oligonucleotides were detected at the single molecule level with high S/N and FRET efficiency. In addtion, the inter-dye diatance of a single donor-acceptor pair could be calculated precisely through smFRET.

Experimental

Reagents and Materials

Sylgard 184 silicone elastomer kit was purchased from Dow Corning, U.S.A. Optical detergent (elc A25) was purchased from Tegent Scientific Ltd. Coverslips (0.13–0.17 mm thick) were purchased from Thermo Fisher Scientific. Cy3- and Cy5-labeled oligonucleotides, 5′-Cy3-ATATATTATTCCCTA-(biotin)-3′ and 5′-Cy5-TAGGGAATAATATAT-3′, were synthesized by Sangon Biotech (Shanghai). APTES was purchased from Aladdin. Sulfo-NHS-biotin was purchased from Sangon Biotech (Shanghai). Streptavidin (STV) was purchased from Amresco. PBS (10 mM, pH 7.4), D-gluocose, gluocose oxidase, catalase, and trolox were purchased from Sigma Aldrich. Ultrapure water (18.2 $M\Omega.cm^{-1}$, Milli-Q Academic, Merck) was used throughout the experiment.

Instrument

Single-molecule fluorescence detection was conducted under objective type of total internal reflection fluorescence microscope (TIRFM, IX81, Olympus, Japan) equipped with a high sensitive EMCCD (Evolve 512 Delta, Photometrics, America). A Dual-view™ imager (Photometrics) was inserted between microscope and EMCCD for imaging of dual-color fluorescence. With the proper Dual-view™ filter set (Cy3 barrier filter 585 nm, Cy5 barrier filter 680 nm), the signals of Cy3 and Cy5 were separated well with minimal crosstalk. The schematic diagram of the setup based on TIRFM was illustrated as Fig. 1.

Elimination of Fluorescence Impurities

Coverslips were cleaned as described by others [42, 43] with some modifications. In brief, the coverslips were immersed in elc A25 (1 %, v/v) and sonicated for 15 min. The cleaned coverslips were transferred to piranha solution (H_2SO_4: H_2O_2=3:1, v/v), and sonicated for about 15–20 min after cooling down to room temperature. Next, the coverslips were flushed with ethanol and water several times, and dried with nitrogen gas.

Identification of Single-Molecule Fluorescence

SMD was conducted on coverslips modified with 1 % (v/v) APTES using a T-type microfluidic with three inlets and one outlet (as shown in Fig. 2). Dye-labeled ssDNA and PBS buffer served as the dispersed phase, and hexadecane with 1 % span 80 (v/v) as the continuous phase. The exposure time was 100 ms, and the enhanced value of EMCCD was set to 240.

Signal to Noise Ratio Analysis

In order to obtain unambiguous single-molecule fluorescence, it is necessary to decrease the background of the sample in order to enhance S/N. The intensity of background fluorescence was subtracted throughout all of the fluorescence intensity analyses.

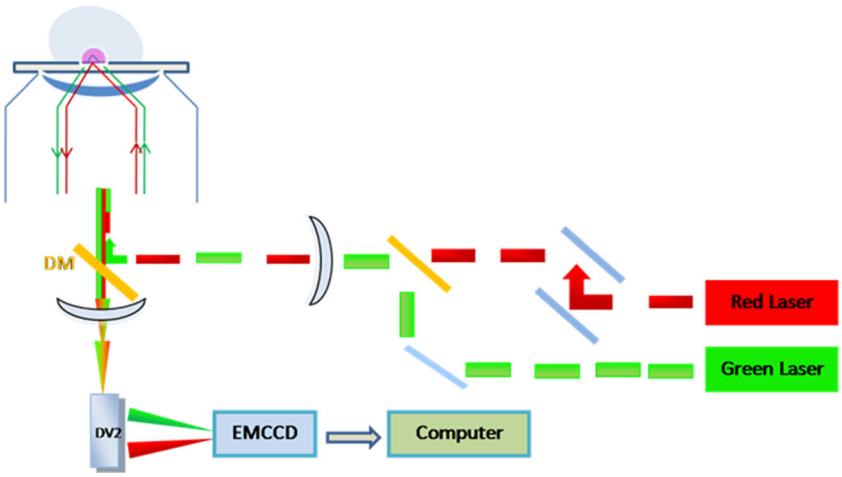

Fig. 1 Schematic diagram of single-molecule dual-color imaging system including an objective type of TIRFM, a green-red laser combiner, and a Dual-view™ imager

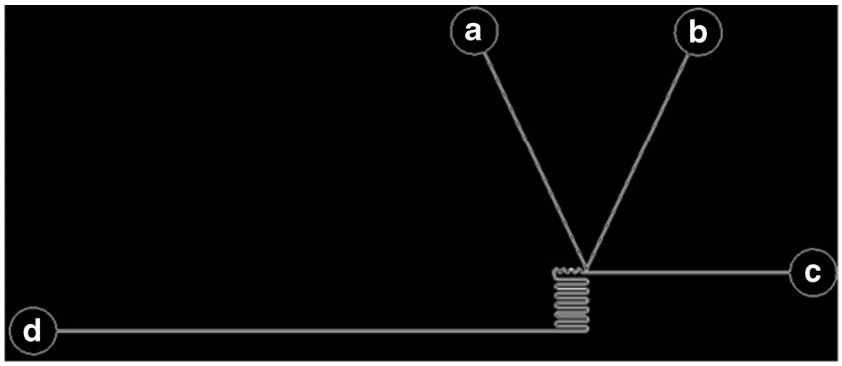

Fig. 2 Structure chart of microfluidic with three inlets **a**, **b**, and **c** and one outlet **d**. A and B served as dispersed phases, and C as continuous phase. The width and depth of channel were 50 μm

Single-Molecule Fluorecence Resonance Energy Transfer (smFRET)

Cy3- and Cy5-labeled ssDNAs were hybridized through heating at 94 °C for 3 min, then cooling down to room temperature slowly. During smFRET, the 532 nm laser that excites Cy3 was turned on and the 635 nm laser exciting Cy5 was only used to confirm the presence of Cy5 molecules. The dual-view imaging system was used to record smFRET.

DsDNA (15 bp) with one strand modified with biotin at one end was immobilized on the substrate through biotin-streptavidin interaction, and smFRET was conducted as illustrated in scheme 1. In brief, the sample chamber was prepared by coupling a coverslip with a PDMS chip (one inlet and one outlet) through plasma treatment. First, APTES (1 %, v/v) was introduced into the channel to coat the coverslip. Then 1 mg/ml sulfo-NHS-Biotin was injected into the channel, followed by introduction of 0.25 mg/ml STV. Finally, 50–100 pM biotinylated duplex DNA with a single donor-acceptor pair was injected to interact with STV. In each step of the procedure, the reagents were incubated for 5–15 min at room temperature, and the channel was flushed with PBS buffer. In order to minimize photobleaching, smFRET was imaged in the presence of an oxygen scavenger system with triplet quencher containing 0.8 % (w/v) D-gluocose, 1 mg/mL glucose oxidase, 0.04 mg/mL catalase, and 2 mM trolox [40, 44].

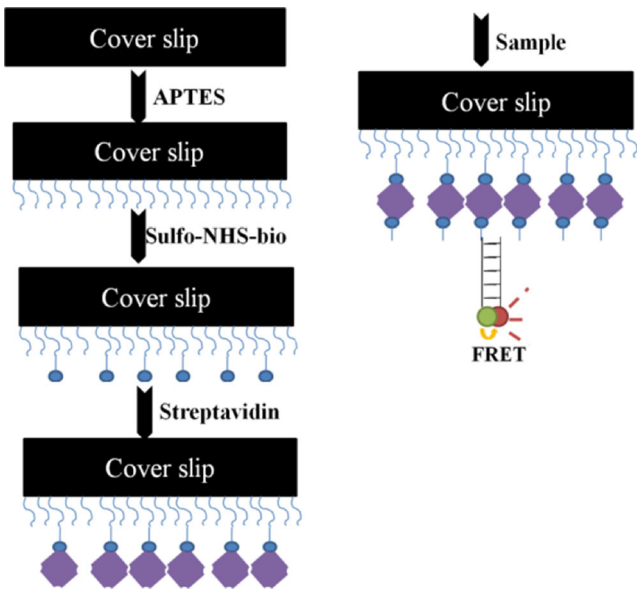

Scheme 1 Schematic diagram of single-molecule fluorescence resonance energy transfer (smFRET)

Alternatively, smFRET was conducted in a T-type microfluidic (Fig. 2). Cy3- and Cy5-labeled ssDNA served as disperse phases, and hexadecane with 1 % span 80 (v/v) as continuous phase. Complementary dye-labeled ssDNAs were encapsulated and hybridized in droplets.

The FRET efficiency was calculated using $E = \frac{I_A}{I_A + I_D}$. Where E represented the FRET efficiency. I_A was defined as fluorescence intensity of the acceptor, and I_D was fluorescence intensity of the donor [39]. The distance of donor and acceptor was calculated using $R = R_0 \sqrt[6]{\frac{1}{E} - 1}$. Where R represented the distance between donor and acceptor, and R_0 was defined as Foster radius [37], which is about 6 nm for Cy3 and Cy5 [45].

Results and Discussion

Elimination of Fluorescence Impurities on Coverslips

As shown in Fig. 3a, we detected several fluorescence spots on coverslips prepared according to previously reported methods [42, 43]. Thus, we used an optical detergent to clean the coverslips followed by sonication in piranha solution. This procedure significantly decreased the surface impurities (Fig. 3b). We tested other approaches to decrease background fluorescence, including filtration of buffer and prebleaching of coverslips, but found this technique most effective (data not shown).

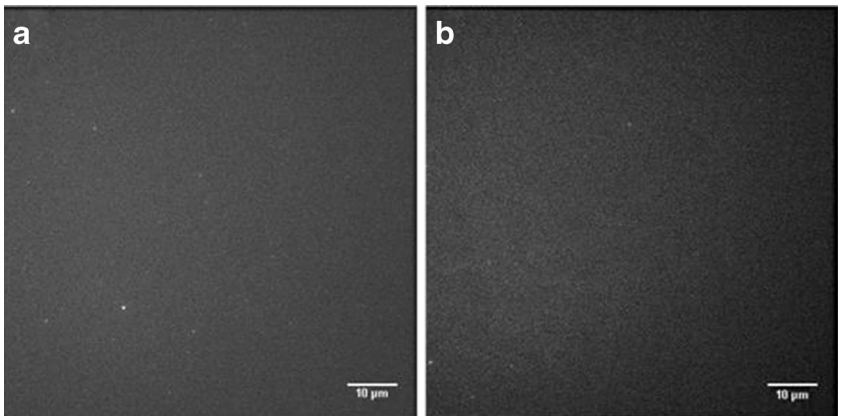

Fig. 3 Images of coverslips cleared by piranha solution without **a** and with **b** optical detergent

Detection of Single-Molecule Fluorescence on Glass Substrate

SMD on Glass Substrate

A 532 nm and a 635 nm laser were applied to excite Cy3 and Cy5, respectively. Cy3 (Fig. 4a) and Cy5 (Fig. 4b) at different concentrations were deposited on APTES-modified coverslips through electrostatic adsorption, and the number of fluorescence spots increased linearly with increased concentration (Fig. 4c).

It is important to determine if observed fluorescence spots contain only one molecule or two or more. This cannot be reliably determined from the fluorescence image itself. Generally, photobleaching of a fluorescing spot containing a single molecule should occur in a single step rather than two or more [46, 47]. Stack images of Cy3 and Cy5 were recorded by using

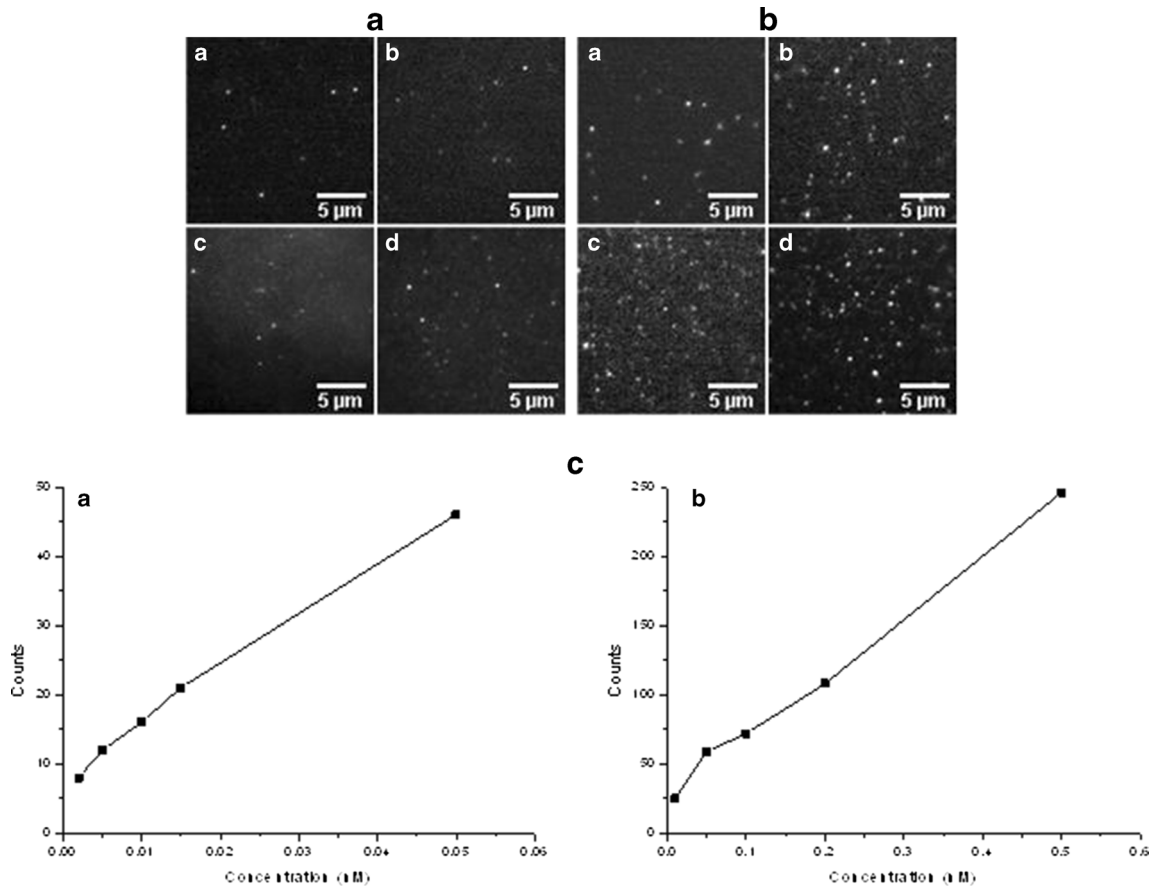

Fig. 4 Fluorescence images of Cy3 and Cy5 at different concentrations. **a**, a-d are representive images of Cy3 concentrations of 0.002, 0.005, 0.015, and 0.05 nM, respectively. **b**, a-d are representive images of Cy5 concentrations of 0.01, 0.05, 0.1, and 0.2 nM, respectively. **c**, Relationship between the number of fluorescence spots and the concentrations of fluorescence molecules. Left and right represent Cy3 and Cy5, respectively

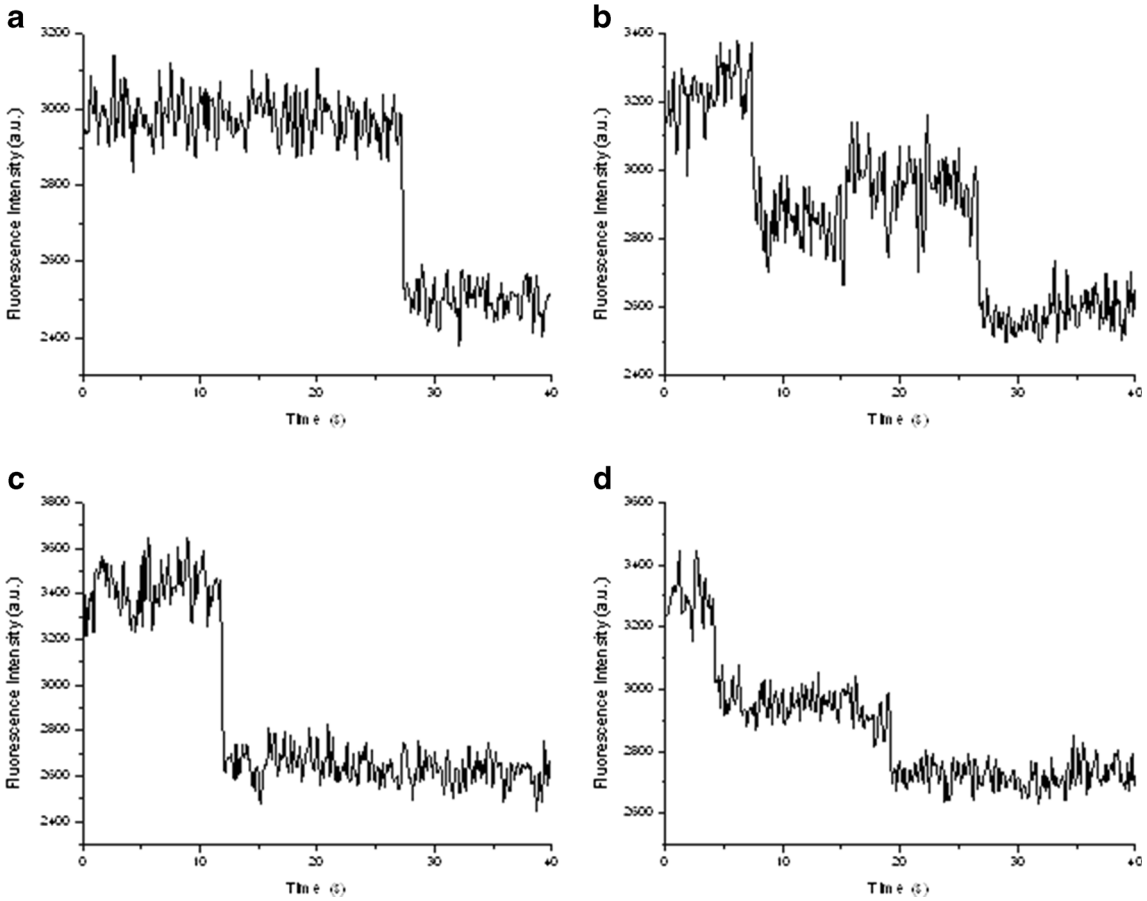

Fig. 5 Photobleach curves of fluorescence molecules. **a** and **b** represent single and multi-step photobleaching of Cy3, **c** and **d** represent single and multi-step photobleaching of Cy5, respectively. The laser power of 532 and 635 nm was about 0.45 mW

EMCCD. Figure 5 shows the fluorescence intensities of fluorescence spots during 300 continuous frames. Photobleaching of observed single fluorescence spots did not all occurr in a single step. In the experiment, 145 single fluorescence spots of each dye were selected randomly. For the Cy3 molecules, one hundred and thirty-seven (~94.5 %) fluorescence molecules were photobleached in a single step while the rest were in two or multiple steps. For Cy5, one hundred and thirty-eight (~95.2 %) fluorescence molecules showed photobleaching in a single step, and the others in two or multiple steps. The results illustrated around 95 % of the Cy3 and Cy5 fluorescence spots were single fluorescence molecules.

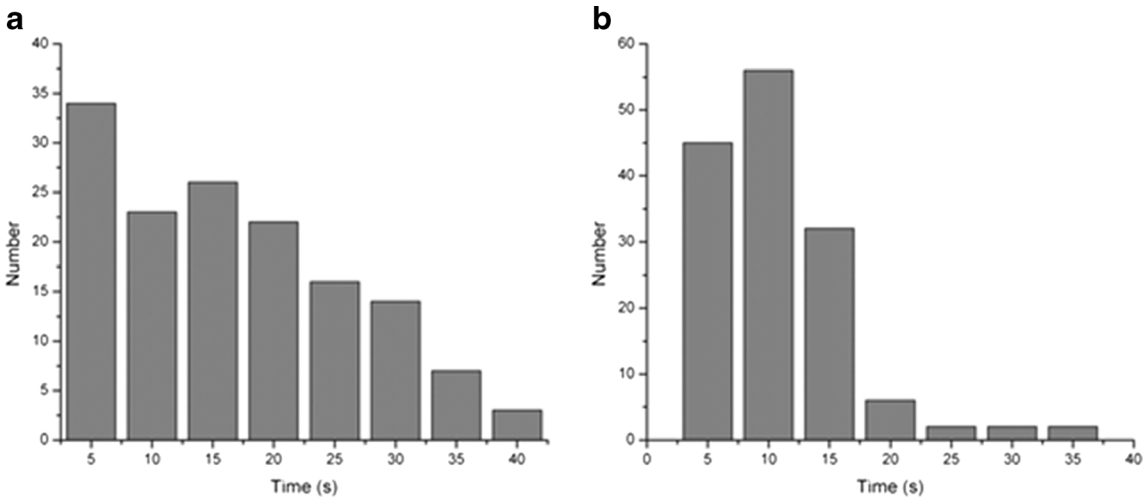

Fig. 6 Distribution of time required for photobleaching of Cy3 **a** and Cy5 **b** fluorescence molecules on substrate at the laser power of 0.45 mW

Statistics of time distribution for photobleaching of Cy3 and Cy5 fluorescence molecules are illustrated in Fig. 6. The average time for Cy3 photobleaching (14.32±0.91 s) was longer than for Cy5 (8.32±0.91 s).

smFRET Immobilized on Substrates

As illustrated in scheme 1, the protocol of smFRET on glass substrates used a stepwise reagent depositon to keep the sample from drying and allow proper concentration for imaging. As shown in Fig. 7a, dually labeled DNA with Cy3 and Cy5 was adsorbed on modified glass substrate and images were obtained with TIRFM. In Cy3 and Cy5 channels, there were several green and red spots, respectively. The two color images were overlaid to generate the composite image (right). Representative single-molecule time trajectories obtained from yellow spot are illustrated in Fig. 7b; the negative correlation of fluorescence intensities between donor and acceptor indicated FRET occurrence. The fluorescence intensity of Cy5 showed a sudden drop at about 20 s, which corresponded to photobleaching of the acceptor, at which point the fluorescense intensity of Cy3 increased. At about 36 s, the fluorescence intensity of Cy3 dropped down, indicating photobleaching of the donor.

Figure 7c shows the FRET efficiency over time based on Fig. 7b. FRET efficiency measured from different donor-

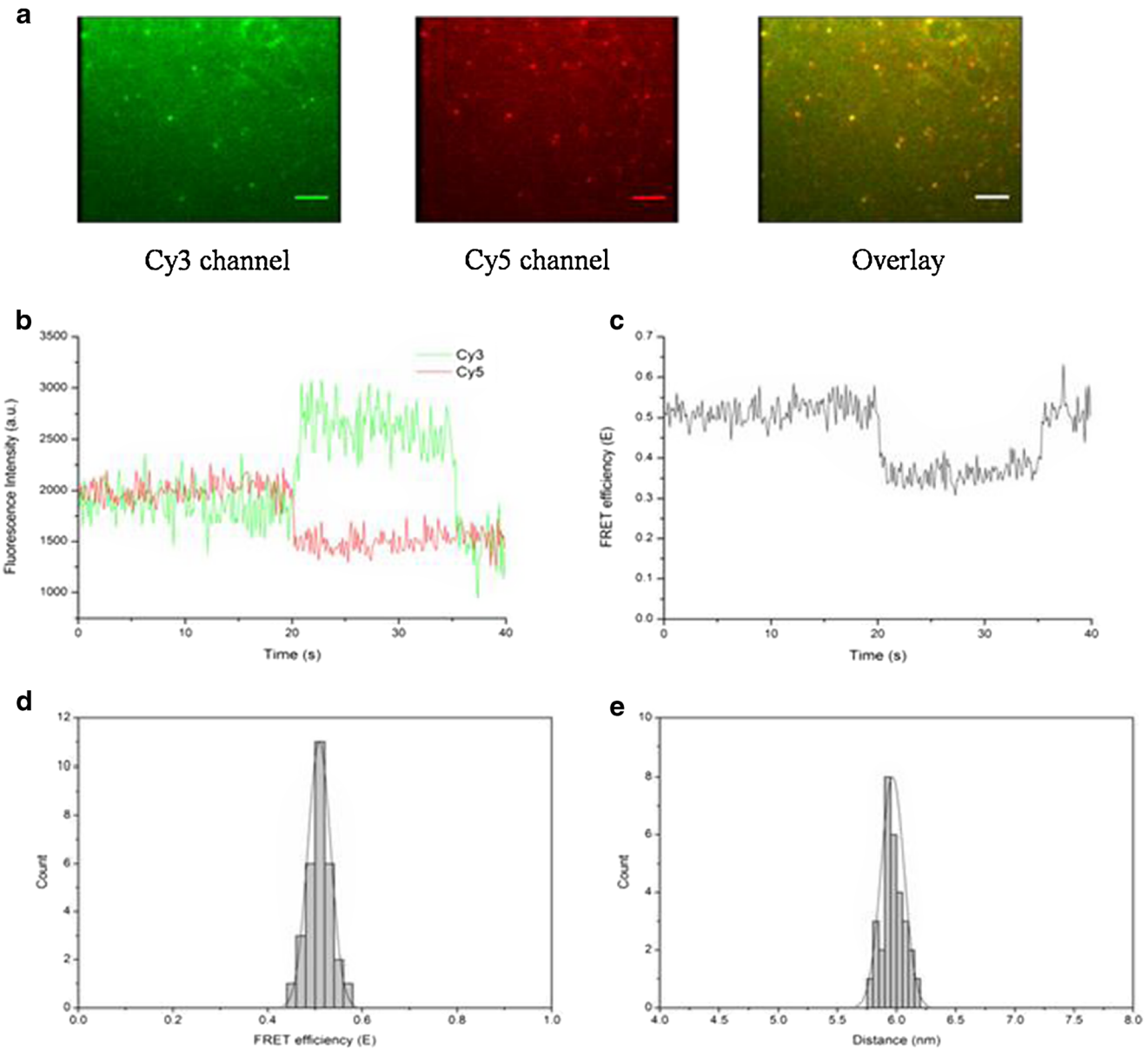

Fig. 7 FRET analysis of Cy3 and Cy5 immobilized on glass substrate. **a** Fluorescence images obtained with TIRFM under excitation of Cy3 only. **b** Single-molecule time trajectories of fluorescence intensities for Cy3 and Cy5. **c** FRET efficiency of **b. d** Histogram distribution of the summarized FRET efficiencies. **e** Donor-acceptor distance histogram distribution calculated based on values in **d**. The scale bar was 5 μm

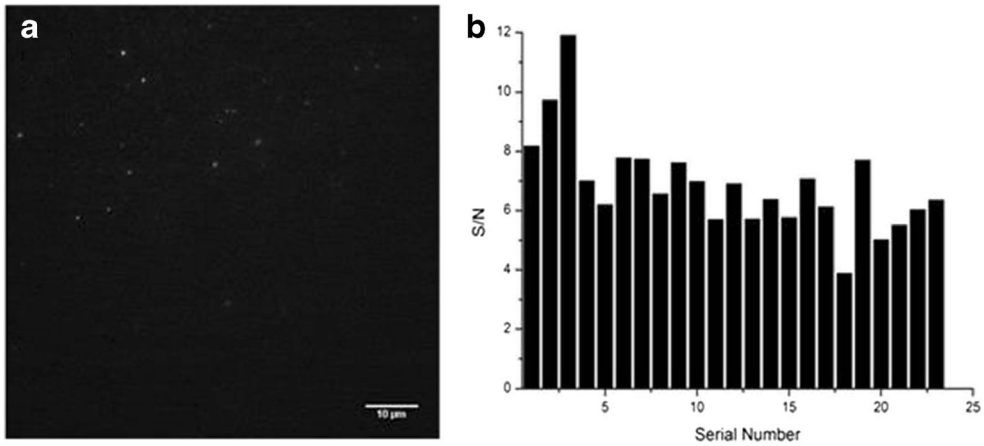

Fig. 8 Signal to noise ratio of fluorescence molecules. **a** Fluorescence spots obtained through objective TIRFM. **b** Distribution of S/N calculated from fluorescence spots after the background intensity was subtracted

acceptor fluorescence spots exhibited normal distribution with a mean value of 0.51±0.03 (Fig. 7d). The distance of donor and acceptor could be calculated based on FRET efficiency (E) and Forster radius (R_0) using the given equation (Fig. 7e). The distances were determined to follow a normal distribution with a mean value of 5.95±0.30 nm.

Signal to Noise Ratio Analysis

In order to interpret fluorescence images, it is necessary to maximize S/N. As shown in Fig. 8a, single fluorescence spots dispersed well on the substrate surface. Figure 8b showed S/N of 23 fluorescence molecules from the image shown in Fig. 8a. The maximum S/N was 11.9, the minimum 3.9, and the mean 6.9±0.34 (much higher than 3.0). The result indicated favourable S/N for single-molecule fluorescence analysis.

Detection of Single-Molecule Fluorescence in Droplets

SMD in Droplets

Single Cy3 and Cy5 fluorescence molecules were encapsulated in droplets (Fig. 9). On excitation, Cy3 and Cy5 could be observed as green (Fig. 9a) and red (Fig. 9d)

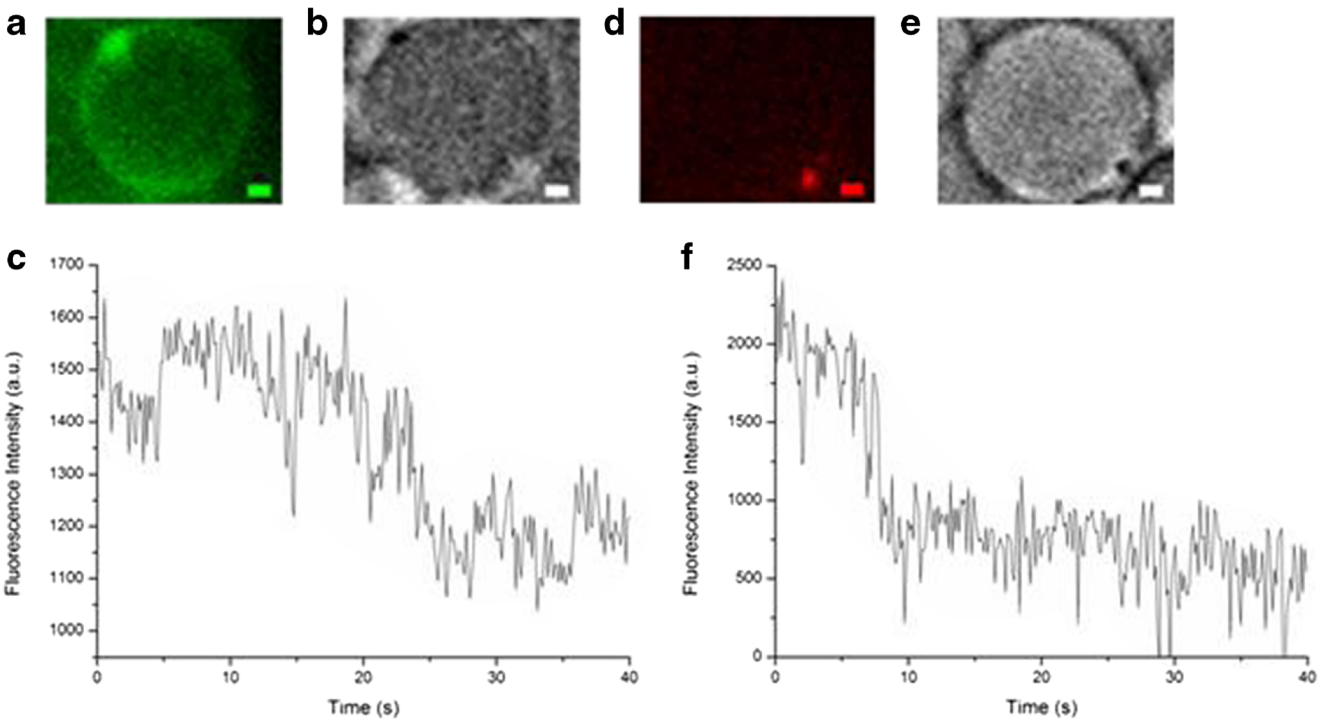

Fig. 9 Detection of single-molecule fluorescence in droplets. **a** and **d**, Fluorescent field images of a single Cy3 and Cy5 molecule encapsulated in droplets. **b** and **e**, Bright field images of the droplets in **a** and **d**, respectively. **c** and **f**, the fluorescence intensity trajectories for a single Cy3 and Cy5 molecule. The scale bar was 1 μm

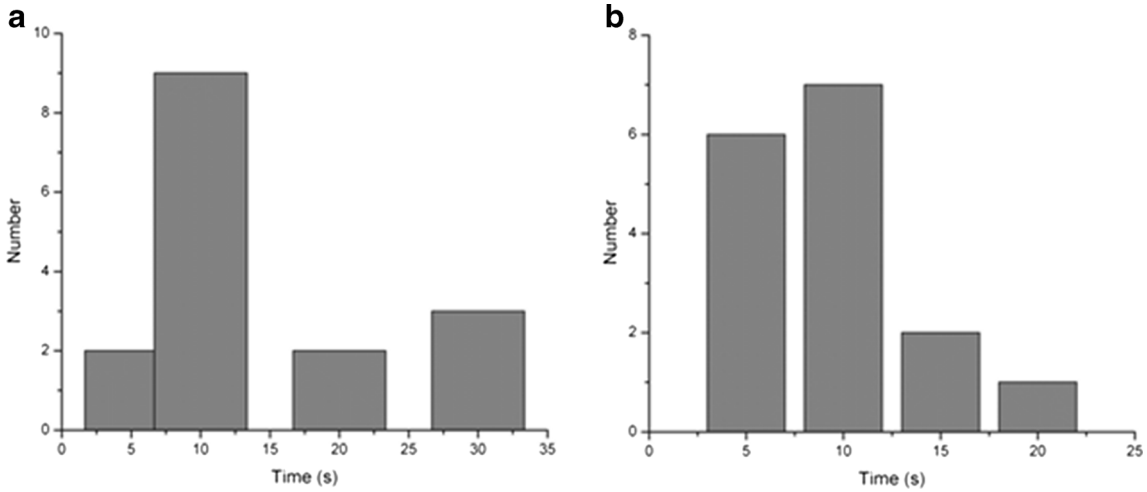

Fig. 10 Histograms of phtobleaching time for Cy3 **a** and Cy5 **b** in droplets at the laser power of 0.45 mW

fluorescence spots, respectively, which appeared as black spots under the bright field (Fig. 9b and e). We observed that nearly all the fluorescence spots were located at the water/air interface of droplets, possibly due to certain absorptive effects. Single step photobleaching curves confirmed that the fluorescence spots encapsulated in droplets were single Cy3 (Fig. 9c) or Cy5 (Fig. 9f) molecule. The fluorescence intensity of Cy3 dropped sharply at about 23 s, while Cy5 at about 8 s.

Figure 10 shows the time distributions for photobleaching of Cy3 and Cy5 molecules encapsulated in droplets. The mean time for photobleaching of Cy3 was 13.48±0.20 s, and for Cy5 8.12±0.20 s, which were comparable with those measured from fluorophores immobilized on substrates.

smFRET in Droplets

To enhance mixing of Cy3 and Cy5 solutions in the microchannel, a winding channel was designed and tested (Fig. 11). We found that this channel allowed better mixing of the solutions in droplets compared to the straight channel. This was confirmed by performing a series of flow rate ratios of continuous and dispersed phase (data not shown).

Hybridization between two complementary ssDNAs took about 1–2 h both on substrate or in static solution, however, previous reports that such hybridization could be completed much faster in fluidic flow or microdroplets [41, 48, 49] at room temperature. Figure 12 shows smFRET of droplets generated through a T-type microfluidic as illustrated in Fig. 11b. The images of single Cy3 and Cy5 molecules were acquired through fluorescent fields (Fig. 12a). Within the view of Dual view™ imaging system, a single fluorescence spot was observed in the Cy5 view channel when the sample was excited solely by 532 nm laser, an indicative of FRET ("Cy5 channel" in Fig. 12a). The yellow spot in the composite image ("Overlay" in Fig. 12a) confirmed occurrence of FRET as well. The negative correlation of fluorescence intensities between donor and acceptor is illustrated in Fig. 12b. During the first 4 s, the fluorescence intensity of Cy5 was much higher than Cy3, which indicated a high FRET efficiency (more than 0.6, seen in Fig. 12c). Then, a sudden drop in Cy5 intensity was accompanied by a sharp rise of Cy3 intensity. At about 26 s, the fluorescence intensity of Cy3 declined due to

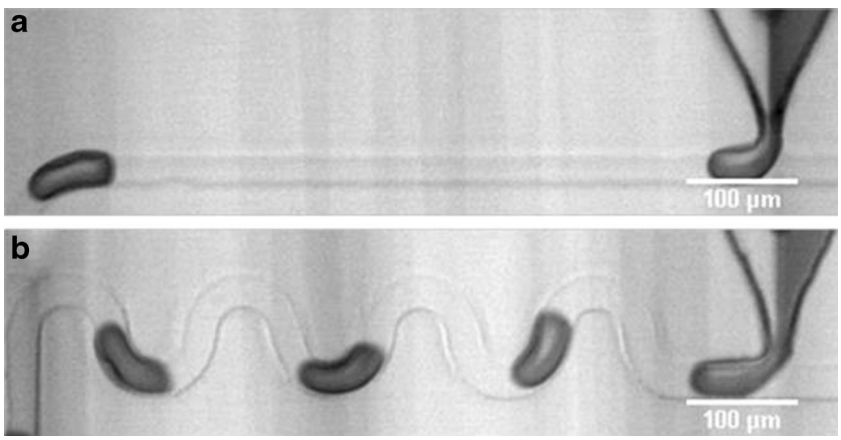

Fig. 11 Water in oil droplets were generated through a T-type microfluidic with straight **a** or winding **b** channels. The gray and transparent solutions were red food dye solution and water, respectively. The flow rates of continuous and disperse phases were 5, 0.5, and 0.5 μL/min. The exposure time was 0.1 ms

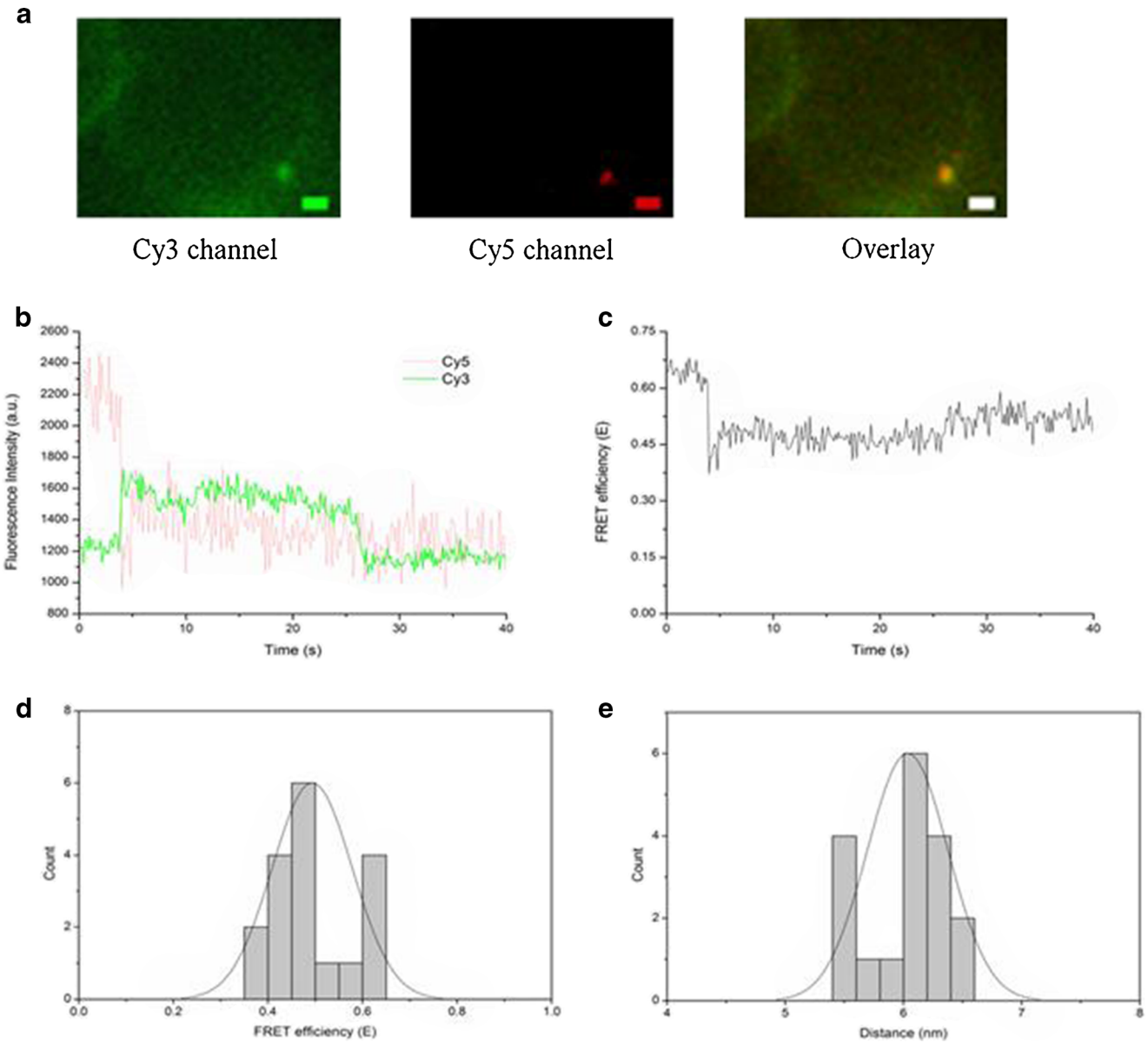

Fig. 12 A representative FRET of a single donor-acceptor pair of Cy3 and Cy5 in a droplet. **a** Fluorescence images under Cy3 excitation. **b** Single-molecule time trajectories of fluorescence intensities of Cy3 and Cy5. **c** FRET efficiency of (b). **d** Histogram distribution from summarized FRET efficiencies. **e** Histogram distribution of distances between donor and acceptor calculated based on **d**. The scale bar was 1 μm

photobleaching. FRET efficiencies acquired from different fluorescence spots followed a normal distribution with a mean value of 0.49±0.03 (Fig. 12d). The distances between donor and acceptor were calculated based on FRET efficiencies of Fig. 12d, with an average value of 6.04±0.15 nm (Fig. 12e).

Conclusions

The detection of single-molecule fluorescence requires improvements to the S/N to obtain unambiguous sample spots. TIRFM with an evanescent wave of less than 200 nm showed excellent features for SMD. The results showed that more than 90 % of the fluorescence spots were single molecules as confirmed by single-step photobleaching. Photobleaching of Cy5 occured more quickly than that of Cy3, consistent with previous results [50, 51]. smFRET was investigated using Cy3 and Cy5 as the donor-acceptor pair with a TIRFM system. The excitation spectral separation is large (~100 nm) and both fluorophores are relatively photostable in an oxygen-free environment [40, 51].

SMD was conducted through both immobilization of target molecules on substrate surface and encapsulation of the target molecules in microdroplets formed in a microfluidic channel. In the former, samples were deposited on APTES-modified substrate through electrostatic or biotin-STV interaction. In

the latter, dye-labeled oligonucleotides were injected into microfluidic channel and encapsulated in single droplets for detection. The results showed that the smFRET microscopic imaging system could detect FRET at the single molecule level, and determine the distance between donor and acceptor precisely. There are several critical factors for smFRET imaging, such as concentration of sample and deposition agents, incubation time and photostability of fluorescence molecules.

In this work, the FRET pair of Cy3 and Cy5 were used to label two ssDNAs with a separation of 15 bases, which should correspond to a contour length of about 5.1 nm for B-form DNA. However, the calculated distances between these fluorophores were 5.95±0.30 and 6.04±0.15 nm when the target molecule were immobilized on substrates and encapsulated in droplets, respectively. This discrepancy (~1 nm) may be due to the orientation and arm sizes of the labeled dyes, which are two important factors for short DNAs [37].

Acknowledgments This work is supported by the State High-Tech Research and Development Plan (863) (grant No. 2012AA02A104) and Foundation for Innovation in Science and Technology, Shanghai Jiao Tong University.

References

1. Soper SA, Shera EB, Martin JC, Jett JH, Hahn JH, Nutter HL, Keller RA (1991) Single-molecule detection of Rhodamine 6G in ethanolic solutions using continuous wave laser excitation. Anal Chem 63(5):432–437
2. Keller RA, Ambrose WP, Goodwin PM, Jett JH, Martin JC, Wu M (1996) Single-molecule fluorescence analysis in solution. Appl Spectrosc 50(7):12A–32A
3. Nie S, Chiu DT, Zare RN (1994) Probing individual molecules with confocal fluorescence microscopy. Science 266(5187):1018–1021
4. Liu C, Qu Y, Luo Y, Fang N (2011) Recent advances in single-molecule detection on micro- and nano-fluidic devices. Electrophoresis 32(23):3308–3318
5. Rotman B (1961) Measurement of activity of single molecules of β-D-galactosidase. Proc Natl Acad Sci U S A 47(12):1981–1991
6. Schmidt T, Schütz G, Baumgartner W, Gruber H, Schindler H (1996) Imaging of single molecule diffusion. Proc Natl Acad Sci 93(7):2926–2929
7. Hanley DC, Harris JM (2001) Quantitative dosing of surfaces with fluorescent molecules: characterization of fractional monolayer coverages by counting single molecules. Anal Chem 73(21): 5030–5037
8. Lord SJ, Lee H-l D, Moerner W (2010) Single-molecule spectroscopy and imaging of biomolecules in living cells. Anal Chem 82(6): 2192–2203
9. Jung G, Wiehler J, Göhde W, Basché T, Steipe B, Bräuchle C (1998) Confocal microscopy of single molecules of the green fluorescent protein. Bioimaging 6(1):54–61
10. Chao SY, Ho YP, Bailey VJ, Wang TH (2007) Quantification of low concentrations of DNA using single molecule detection and velocity measurement in a microchannel. J Fluoresc 17(6):767–774
11. Rust MJ, Bates M, Zhuang XW (2006) Sub-diffraction-limit imaging by stochastic optical reconstruction microscopy (STORM). Nat Methods 3(10):793–795
12. Huang B, Babcock H, Zhuang XW (2010) Breaking the diffraction barrier: super-resolution imaging of cells. Cell 143(7):1047–1058
13. Bates M, Jones SA, Zhuang XW (2013) Stochastic optical reconstruction microscopy (STORM): a method for superresolution fluorescence imaging. Cold Spring Harb Protoc 2013(6):498–520
14. Huang B, Wang W, Bates M, Zhuang X (2008) Three-dimensional super-resolution imaging by stochastic optical reconstruction microscopy. Science 319(5864):810–813
15. Clegg RM, Murchie AI, Zechel A, Carlberg C, Diekmann S, Lilley DM (1992) Fluorescence resonance energy transfer analysis of the structure of the four-way DNA junction. Biochemistry 31(20): 4846–4856
16. Clegg RM, Murchie A, Zechel A, Lilley D (1993) Observing the helical geometry of double-stranded DNA in solution by fluorescence resonance energy transfer. Proc Natl Acad Sci 90(7):2994–2998
17. Klostermeier D, Millar DP (2001) RNA conformation and folding studied with fluorescence resonance energy transfer. Methods 23(3):240–254
18. Walter NG (2001) Structural dynamics of catalytic RNA highlighted by fluorescence resonance energy transfer. Methods 25(1):19–30
19. Sekar RB, Periasamy A (2003) Fluorescence resonance energy transfer (FRET) microscopy imaging of live cell protein localizations. J Cell Biol 160(5):629–633
20. Sorkin A, McClure M, Huang F, Carter R (2000) Interaction of EGF receptor and Grb2 in living cells visualized by fluorescence resonance energy transfer (FRET) microscopy. Curr Biol 10(21): 1395–1398
21. Ishii Y, Yoshida T, Funatsu T, Wazawa T, Yanagida T (1999) Fluorescence resonance energy transfer between single fluorophores attached to a coiled-coil protein in aqueous solution. Chem Phys 247(1):163–173
22. Ha T, Enderle T, Ogletree D, Chemla D, Selvin P, Weiss S (1996) Probing the interaction between two single molecules: fluorescence resonance energy transfer between a single donor and a single acceptor. Proc Natl Acad Sci 93(13):6264–6268
23. Hirschfeld T (1976) Optical microscopic observation of single small molecules. Appl Opt 15(12):2965–2966
24. Castro A, Fairfield FR, Shera EB (1993) Fluorescence detection and size measurement of single DNA molecules. Anal Chem 65(7):849–852
25. Xu X-H, Yeung ES (1997) Direct measurement of single-molecule diffusion and photodecomposition in free solution. Science 275(5303):1106–1109
26. Zheng HZ, Pang DW, Lu ZX, Zhang ZL, Xie ZX (2004) Combing DNA on CTAB-coated surfaces. Biophys Chem 112(1):27–33
27. Kurita H, Torii K, Yasuda H, Takashima K, Katsura S, Mizuno A (2009) The effect of physical form of DNA on exonucleaseIII activity revealed by single-molecule observations. J Fluoresc 19(1): 33–40
28. Kang SH, Lee S, Yeung ES (2010) Digestion of individual DNA molecules by lambda-exonuclease at liquid–solid interface. Analyst 135(7):1759–1764
29. Ueda M, Sako Y, Tanaka T, Devreotes P, Yanagida T (2001) Single-molecule analysis of chemotactic signaling in Dictyostelium cells. Science 294(5543):864–867
30. Elf J, Li G-W, Xie XS (2007) Probing transcription factor dynamics at the single-molecule level in a living cell. Science 316(5828): 1191–1194
31. Knemeyer J-P, Herten D-P, Sauer M (2003) Detection and identification of single molecules in living cells using spectrally resolved fluorescence lifetime imaging microscopy. Anal Chem 75(9):2147–2153
32. Seemann R, Brinkmann M, Pfohl T, Herminghaus S (2012) Droplet based microfluidics. Rep Prog Phys 75(1):1–41

33. Whitten WB, Ramsey JM, Arnold S, Bronk BV (1991) Single-molecule detection limits in levitated microdroplets. Anal Chem 63(10):1027–1031
34. Barnes MD, Ng KC, Whitten WB, Ramsey JM (1993) Detection of single rhodamine 6G molecules in levitated microdroplets. Anal Chem 65(17):2360–2365
35. Reiner JE, Crawford AM, Kishore RB, Goldner LS, Helmerson K, Gilson MK (2006) Optically trapped aqueous droplets for single molecule studies. Appl Phys Lett 89(1):1–4
36. Yasuda M, Iida A, Ito S, Miyasaka H (2012) Fluorescence detection of single guest molecules in ultrasmall droplets of nonpolar solvent. Phys Chem Chem Phys 14(1):345–352
37. Zhang H, Shu D, Browne M, Guo P (2010) Construction of a laser combiner for dual fluorescent single molecule imaging of pRNA of phi29 DNA packaging motor. Biomed Microdevices 12(1):97–106
38. Joo C, Ha T (2012) Single-molecule FRET with total internal reflection microscopy. Cold Spring Harb Protoc 2012(12): pdb.top072058
39. Lee W, von Hippel PH, Marcus AH (2014) Internally labeled Cy3/Cy5 DNA constructs show greatly enhanced photo-stability in single-molecule FRET experiments. Nucleic Acids Res 1–11
40. Kim S-H, Choi D-S, Kim D-S (2008) Single-molecule detection of fluorescence resonance energy transfer using confocal microscopy. J Opt Soc Korea 12(2):107–111
41. Reiner JE, Crawford AM, Kishore RB, Goldner LS, Helmerson K, Gilson MK (2006) Optically trapped aqueous droplets for single molecule studies. Appl Phys Lett 89(1):013904
42. Jin XY, Jin XF, Ding YJ, Jiang JH, Shen GL, Yu RQ (2008) A piezoelectric immunosensor based on agglutination reaction with amplification of silica nanoparticles. Chin J Chem 26(12):2191–2196
43. Wu HX, Dong SQ, Kang JW, Lu XQ (2008) Electrochemical behavior of ascorbic acid on hexaaza macrocyclic copper (II) complex modified Au electrode and its analytical application. Chin J Chem 26(10):1893–1898
44. Rasnik I, McKinney SA, Ha T (2006) Nonblinking and long-lasting single-molecule fluorescence imaging. Nat Methods 3(11):891–893
45. Joo C, Ha T (2012) Preparing sample chambers for single-molecule FRET. Cold Spring Harb Protoc 2012(10):1104–1108
46. Xia T, Li N, Fang X (2013) Single-molecule fluorescence imaging in living cells. Annu Rev Phys Chem 64:459–480
47. Funatsu T, Harada Y, Tokunaga M, Saito K, Yanagida T (1995) Imaging of single fluorescent molecules and individual ATP turnovers by single myosin molecules in aqueous solution. Nature 374(6522):555–559
48. Yea KH, Lee S, Choo J, Oh CH (2006) Fast and sensitive analysis of DNA hybridization in a PDMS micro-fluidic channel using fluorescence resonance energy transfer. Chem Commun (Camb) 14:1509–1511
49. Kim S, Chen L, Lee S, Seong GH, Choo J, Lee EK, Oh C-H, Lee S (2007) Rapid DNA hybridization analysis using a PDMS microfluidic sensor and a molecular beacon. Anal Sci 23(4):401–406
50. Aitken CE, Marshall RA, Puglisi JD (2008) An oxygen scavenging system for improvement of dye stability in single-molecule fluorescence experiments. Biophys J 94(5):1826–1835
51. Joo C, Ha T (2012) Single-molecule FRET with total internal reflection microscopy. Cold Spring Harb Protoc 2012:1223–1237